Nat. Hazards Earth Syst. Sci. Discuss., 3, 3251–3286, 2015
www.nat-hazards-earth-syst-sci-discuss.net/3/3251/2015/
doi:10.5194/nhessd-3-3251-2015

Natural Hazards and Earth System Sciences
Discussions

Variations in water storage in China over recent decade from GRACE Observations and GLDAS

X. Mo[1,2], **J. Wu**[1,2], **Q. Wang**[1,2], **and H. Zhou**[1,2]

[1]Academy of Disaster Reduction and Emergency Management, Ministry of Civil Affairs and Ministry of Education, Beijing Normal University, Beijing, China
[2]Center for Drought and Risk Research, Beijing Normal University, Beijing, China

Received: 7 January 2015 – Accepted: 28 March 2015 – Published: 11 May 2015

Correspondence to: J. Wu (jjwu@bnu.edu.cn)

Published by Copernicus Publications on behalf of the European Geosciences Union.

Abstract

We applied GRACE Tellus products in combination with GLDAS simulations and data from reports, to analyze variations in terrestrial water storage (TWS) in China and eight of its basins from 2003 to 2013. Amplitudes of TWS were well restored after scaling, and showed good correlations with those estimated from models at the basin scale. TWS generally followed variations in annual precipitation, it decreased linearly in Huai River basin ($-0.564\,cm\,yr^{-1}$) and increased with fluctuations in Changjiang River basin ($0.348\,cm\,yr^{-1}$), Zhujiang basin ($0.552\,cm\,yr^{-1}$) and Southeast Rivers basin ($0.696\,cm\,yr^{-1}$). In Hai River basin and Yellow River basin, groundwater exploitation may have altered TWS's response to climate, but it began to restore since 2012. Changes in soil moisture storage contributed over 50 % in of variances in TWS in most basins. Precipitation and runoff showed large impact on TWS, with explained variances higher in TWS in the south than in the north. North China and Southwest Rivers region exhibited long-term TWS depletions. TWS increased significantly over the recent decade in the middle and lower reaches of Changjiang, southeastern coastal area, as well as the Hoh Xil, and headstream region of the Yellow River in Tibetan plateau. The findings in this study could be helpful to climate change impact research and disaster mitigation planning.

1 Introduction

Terrestrial water storage (TWS) is a key component of global hydrological cycle and plays a critical role in Earth's climate system (Famiglietti et al., 2004). Despite its importance, there are still much gaps in the existing water storage observation networks at both the global and regional scale (Lettenmaier and Famiglietti, 2006). Although recent advances in satellite imaging and altimetry have strengthened our monitoring capability over vast areas, these technologies primarily provide only variation information for single components in TWS, such as precipitation estimates, surface soil moisture,

snow cover, and water level. With the progress in satellite gravimetric techniques, direct observation of TWS has become available. The GRACE twin satellites were launched in 2002 as a joint space mission between NASA (US) and DLR (German) to observe variations in Earth's gravity field. Over land, these observations provide information of integrated water storage changes in the vertical profile, including surface water reservoirs, upper layers of soil and underground water reservoirs.

At global, regional or basin scale, GRACE data have been applied to analyze seasonal cycle characteristics of TWS (Schmidt et al., 2006; Syed et al., 2008; Strassberg et al., 2007), to identify TWS anomalies caused by extreme climate (Andersen et al., 2005; Chen et al., 2009; Long et al., 2013), etc. Because of the lack of direct observations independent to GRACE TWS, TWS estimated from the atmospheric water balance, land water balance and model simulations were used to compare with and verify the GRACE TWS (Yirdaw et al., 2008; Zeng et al., 2008; Syed et al., 2005; Schmidt et al., 2006). These papers have demonstrated that GRACE data are capable of identifying seasonal and long-term variations in TWS and have also made contributions to the development of climate and hydrological models.

GRACE TWS combined with hydrological information from other observations or models could help us further understand and manage variables in the hydrological cycle. Land surface model simulations were used to infer the roles of water components (snow water, canopy water and soil water) in GRACE terrestrial water storage change (TWSC) and to understand the effect of hydrologic fluxes fluctuation on water storage (Syed et al., 2008; Kim et al., 2009). With the help of TRMM data and NOAA's CPC model simulations, Crowley et al. (2008) found that the source (precipitation) is more important than sink (evapotranspiration and runoff) to the water balance in the Amazon basin. Other papers tried to seperate variations in groundwater storage from GRACE TWS, and their results showed agreement with in situ observations (Rodell et al., 2009; Leblanc et al., 2009; Famiglietti et al., 2011; Jin et al., 2013).

In China, GRACE data have been compared with several model simulations and used to extract TWS's spatial and temporal variation characteristics as well as its responses to droughts (Duan et al., 2007; Zhong et al., 2009; Wang et al., 2013; Hu et al., 2006; Xu et al., 2013; Tang et al., 2013, 2014). The serious TWS depletion in North China has gained much attention in recent years (Su et al., 2011; Moiwo et al., 2012; Feng et al., 2013). Previous researches have mostly focused on characteristics of seasonal cycle in TWS in certain regions, and there has been less further analysis of long-term variations over China. Moreover, early researches were typically limited by the short period of data availability and the obsolete version, and leakage errors in TWS from processed GRACE data could also misguide analyses at the regional scale.

China is one of the countries confronted with problems of water scarcity. As populations grow and agriculture and industry expands, the booming demand for fresh water has made this problem more urgent. The knowledge of TWS variations over the recent decade is necessary for understanding the large-scale water storage variation process. In this study, the GRACE Tellus land products and Global Land Data Assimilation System (GLDAS) products, combined with data records from national water resources bulletins, were used to analyze long-term TWS variations in China as well as in its eight major basins. This study could give guidance to water resource management and future research on areas with critical water storage changes in China.

2 Data and methods

2.1 Data

The monthly grids from GRACE Tellus land data are applied to analyze TWS variations. The product is derived from the latest Release 05 spherical harmonics, which is an improvement over the previous 04 version. Several institutions provide gravity solutions, such as the University of Texas Center for Space Research (CSR), NASA's Jet Propulsion Laboratory (JPL), and Deutsches GeoForschungsZentrum (GFZ). A recent comparison suggested that TWS estimates from GFZ, CSR and JPL solutions were highly correlated with one other, and tiny differences among them were within

the margin of solution's error (Sakumura et al., 2014). Among these three products, the one from CSR had the smallest root-mean-square (RMS) of deviations between the ensemble mean and itself in 156 basins around the world. In this study, we chose products derived from CSR's solution for the following analyses. The paper by Swenson et al. (2006) describes the details of the post-processing for the spherical harmonics. The final grid (1° in both latitude and longitude) values are presented in the form of changes in equivalent water thickness (unit: centimeter) relative to a time-mean baseline. The data period is from January 2003 to December 2013 and months of absent data are as follows: June 2003, January and June 2011, May and October 2012, March, August and September 2013. Grid scale factors, corresponding to the gridded product, were used to partially correct leakage errors and restore the amplitude-damping caused by the filtering process. Errors and uncertainties in mass variation can be computed from the scaled gridded data (Launderer et al., 2012). In this paper, gridded fields of scale factors and error estimates provided along with the GRACE Tellus products were calculated following Landerer's method based on NCAR's CLM4 model (Oleson et al., 2008).

Monthly flux/state variables (Table 1) from GLDAS (Rodell et al., 2004a) were applied to estimate water storage variations, and these variables were also used to address variations in the components of water storage. GLDAS drives four land surface models: Mosaic (Koster and Suarez, 1996), Noah (Chen et al., 1996; Koren et al., 1999; Betts et al., 1997; Ek et al., 2003), Community Land Model (CLM) (Bonan et al., 1998; Dickinson et al., 1993; Dai et al., 1997), and Variable Infiltration Capacity (VIC) (Liang et al., 1994, 1996). Satellite-based and ground-based observations are integrated into these models to generate optimal fields of land surface states and fluxes. The forcings for these models from 2001 to present is a combination of NOAA/GDAS atmospheric analysis fields, spatially and temporally disaggregated NOAA Climate Prediction Center Merged Analysis of Precipitation (CMAP) fields (Xie and Arkin, 1996) and observation-based downward shortwave and long wave radiation fields from the Air Force Weather Agency (AFWA).

Drainage networks are mostly distributed in the monsoon dominated Middle and East China (Fig. 1a), which are also highly populated area with high levels of water consumption. In this study, we specifically focus on eight large basins, Heilongjiang River, the Liao River, Hai River, Huai River, Yellow River, Changjiang, Zhujiang, Southeast Rivers (with abbreviations of HLJ, LR, HaiR, HuaiR, YR, CJ, ZJ and SERs, respectively, in the following tables). Desert and Gobi are dominant land covers in northwestern China, while glacier, snow cover and frozen soil are widely distributed across the Tibetan plateau (Fig. 1b). Vector data for desert, glacier and lake are acquired from the Data Sharing Infrastructure of Earth System Science (http://www.geodata.cn). Annual Chinese water resources bulletins from 2003 to 2013 are acquired from the Ministry of Water Resources to assist with the analysis. Values for surface water resources, ground water resources and gross water resources provided in the water resources bulletins are the results of existing monitoring and statistical analyses (Fig. 5). Surface water resources refer to water storage in rivers, lakes and glaciers, and groundwater resources mainly refer to water storage in underground shallow aquifers.

2.2 Methods

2.2.1 Data pre-processing

Unlike scale factor applied for region-averaged TWS time series in previous researches (Rodel et al., 2004b; Chen et al., 2007; Landerer et al., 2010; Feng et al., 2013), monthly products from GRACE Tellus land data were multiplied by grid scale factors to restore signal attenuation. Next, the average value for each grid from January 2003 to December 2013 was subtracted from all other scaled monthly grids. The deviations to time-average TWS were used for the following analyses. At the regional scale, all grids in a basin were averaged with the cosine of latitude as the weight, and missing values from absent months were interpolated from adjacent available months. For regional averaged TWS, total errors were calculated from error fields provided along with the GRACE products (Eqs. (1), (2) and Table 4). Because of spatial correlation among

neighboring grids, covariance was considered in the calculation (Landerer et al., 2012). The dist in Eq. (1) is the geometric distance between any two grids in the basin (unit: km), n is the number of valid grids in a specific basin, β is the de-correlation length, which is set to 300 for measurement error and 100 for leakage error. Early analysis suggested that the TWS variations could be distinguished from GRACE monthly data over regions larger than 200 000 km^2,with an accuracy of 1.5 cm equivalent water thickness (Rodell and Famiglietti, 1999), and the larger the spatial scale of the research area was, the better the accuracy the results could acquire (Swenson et al., 2003; Wahr et al., 2004).

$$\mathrm{Error}_{\mathrm{region}} = \sqrt{\sum_{i=1}^{n}\sum_{j=1}^{n} \mathrm{Error}_i \times \mathrm{Error}_j \times e^{-\left(\mathrm{dist}_{i,j}^2\right)/(2\times\beta^2)}} \Big/ n \quad (1)$$

$$\mathrm{Error}_{\mathrm{total}} = \sqrt{(\mathrm{Error}_{\mathrm{measure}})^2 + (\mathrm{Error}_{\mathrm{leakage}})^2} \quad (2)$$

State variables (snow water equivalent – SWE, canopy water storage – CWS – and total soil moisture storage in all layers – SM) and flux variables (precipitation – P, evapotranspiration – E – and runoff – Q) from the four models in GLDAS were presented in the form of equivalent water thickness (unit: cm). The time averages were removed from these variables following the process used for the GRACE data to keep the same time-base for comparison. The ensemble mean (arithmetic average) of the four models' simulations was also calculated and regarded as the representative of model results.

2.2.2 TWS estimates from model simulations

In despite of deficiencies in model simulations, state variables SWE, CWS and SM from GLDAS outputs can be combined to estimate TWS (Eq. 3). Although the estimates are not able to fully reflect the information in the actual TWS variations, they can still capture the fluctuation and magnitude in land hydrology, which is necessary for assessing and understanding the TWS observation from GRACE (Syed et al., 2004).

$$\mathrm{TWS} = \mathrm{SWE} + \mathrm{CWS} + \mathrm{SM} \quad (3)$$

Correlation coefficients between TWS from scaled GRACE and model simulations are listed in Table 2. TWS estimates from CLM and VIC have relatively poor correlations with GRACE observations at the national scale. However, all model estimates generally have high correlation coefficients at the regional scale, except in Heilongjiang river basin. The differences between models and regions showed that model simulations have a high degree of uncertainties, and TWS estimates from NOAH and the GLDAS ensemble mean have a good agreement with TWS from scaled GRACE at both the national and regional scale. The differences between the GLDAS simulations and the GRACE observations are mainly the result of missing information on components of land hydrology, such as groundwater and reservoirs, and poor parameterization (snow cover, frost soil, etc.) in the model mechanism (Syed et al., 2008). These components or processes could be critical to TWS in some parts of the world (Rodell et al., 2001). The RMS of deviations from ensemble mean was calculated as the bias of TWS estimates from the GLDAS simulations (Table 3).

2.2.3 Scaling effect assessment

To understand how much changes scale factors could make to GRACE TWS in China, we compared the spatial distributions of the amplitude of TWS variations from observations and simulations. The RMS of the time series at each grid was taken as a proxy for local TWS amplitude, and then the empirical probability density distributions (PDF) for RMS values over China were calculated for TWS derived from scaled and unscaled GRACE data and the model simulations. To avoid abnormal values, only RMS values between the 5th and 95th quantile over China were considered. For regional averaged TWS, the slopes and coefficients of determination R^2 were calculated with a linear least square fit to assess the damping influence of leakage errors (Eq. 4).

$$\mathrm{TWS}_{\mathrm{scaled}} = a \times \mathrm{TWS}_{\mathrm{unscaled}} \quad (4)$$

2.2.4 Analysis of TWS long-term variations

TWSC the integrated changes in the vertical components of TWS, is the difference between current and previous months' TWS (Eq. 5). This value can also be inferred using the water balance with precipitation, evapotranspiration and runoff data in a specific basin (Hirschi et al., 2006; Eq. 6). With GLDAS and GRACE products, we applied correlation analysis to find out how much state/flux variables can contribute to TWSC's variance in different basins. After applying a 13-point moving average to remove intra-annual variations in times series, we analyzed annual variations based on the regionally averaged TWS from scaled GRACE and the GLDAS ensemble mean, in combination with annual Chinese water resources bulletins. Annual data from the water resources bulletins were converted from volume (unit: million m^3) to equivalent water thickness (unit: cm), and the multi-year average was removed. To identify major areas with significant TWS increase or depletion in the recent decade, linear trend for each grid was calculated from the scaled GRACE TWS, and the long-term trends of seasonal average TWS were also analyzed.

$$\mathrm{TWSC}_N = \mathrm{TWS}_N - \mathrm{TWS}_{N-1} \quad (5)$$

$$\mathrm{TWSC} = P - E - Q \quad (6)$$

3 Results and discussion

3.1 Effect of the scale factors in China

The effect of the truncation ($\mathrm{Order}_{\max} = 60$) and filtering processes (300 km Gaussian filtering) on the GRACE spherical harmonics is equivalent to a low-pass filter, thus the effective resolution of the GRACE TWS product is several hundred kilometers (Tapley et al., 2004). The TWS time series in a $1^\circ \times 1^\circ$ grid was mixed with TWS signals from surrounding areas, which led to leakage errors. When the outside TWS signal was stronger than the inside one, the grid value was exaggerated by leakage errors and

vice versa. In addition, the sign of gridded TWS could even be changed in cases where inside and outside TWS signals had opposite phases caused by extreme changes in topography, such as in the Turpan basin in northwestern China. As relationships between TWS series at different spatial scales were inferred from land-hydrology model simulations, grid scale factors calculated based on these information could partially correct GRACE TWS and to some extent recover small-scale information (Landerer et al., 2012); thus, these scale factors can be quite helpful for extracting TWS over arbitrary shaped region.

In Fig. 2, spatial difference in the RMS of TWS from scaled GRACE data have been expanded from approximately 6 cm to approximately 12 cm, and the highly left-skewed empirical PDF curve is quite similar to those from the model simulations with for the RMS of the TWS from the unscaled GRACE data, the empirical PDF curve has a different relative peak position around with RMS value of 3 cm. The right boundary of RMS represents a strong TWS amplitude in space, and they are distinct among TWS model estimates' and GRACE observations because differences in the model mechanisms are amplified in TWS active regions. The TWS from the scaled GRACE data, the MOSAIC, VIC, CLM and GLDAS ensemble mean all have a left boundary of RMS close to 0 cm. Spatially, this corresponds to northwest China, which is an arid climate zone with vast deserts (Figs. 1, 3b and c). From the comparison in Fig. 3, we can also see that scaled GRACE TWS has similar distribution of amplitude with that from GLDAS ensemble mean over China, particularly the boundary with RMS of 3 cm, separating arid and humid climate zones. TWS is quite stable over some part of the oceans and major deserts around the world, thus a small RMS for TWS in these areas indicates small data noise in GRACE TWS (Sakumura et al., 2014). Both the empirical PDFs and the spatial distribution of the RMS of the TWS suggested that gridded scale factors could correct the amplitude of TWS in space. Previous research has demonstrated that correction for leakage error is critical to regional TWS analysis (Chen et al., 2014).

Regionally averaged TWS time series from scaled and unscaled GRACE data are highly correlated, and this means that the fluctuation process in TWS has not been

heavily influenced by the scale factors. At the same time, the values of TWS were all amplified to different degrees (Table 4), with the amplitudes in Huai River basin and Zhujiang basin increasing over 50 %. However, in the Liao River basin and Yellow River basin only small changes occurred (< 10 %). The slopes in Table 4 can be regarded as the basin-specific scale factors for GRACE TWS. Generally, basins with large areas are less affected by leakage errors and have slopes close to 1, but geographical location and hydrological cycle characteristics will contribute to this effect, as well.

3.2 Annual variations in regional TWS time series

In general, fluctuations in annual precipitation could appropriately characterize the inter-annual variabilities in regionally averaged TWS, but different processes also exist in certain basins or over certain periods because of the influence of other factors (Figs. 4 and 6). TWS in China was in a relatively positive condition before 2006, but then stayed at a continuously low level with a high variability from 2006 to 2012. During this period, extreme climate disasters occurred frequently and caused particularly sharp declines in TWS in 2007, 2009 and 2011. TWS in China did not recover to the same level in 2005 until 2013. This periodic process was partially reflected in the TWS estimates from the GLDAS ensemble mean (mostly soil moisture storage) but not in the residual series or water resources records (Figs. 4 and 5). This process may be controlled by changes in some large-scale climate processes, which need to be further analyzed in the future.

In Northeast China, TWS observations and simulation estimates in Heilongjiang basin were consistent and showed no long-term trend; the region mainly suffered from two severe regional droughts in 2007 and 2011 and a significant basin flood event in 2013. Annual precipitation in Liao River basin continuously declined from 2005 to 2009 and then increased rapidly in following years; TWS estimates and water resources records both precisely captured this process. Nevertheless, it seemed that the TWS observations failed to respond to heavy precipitation in 2010, with a 9 cm increase in

TWS estimates and only a 3 cm increase in TWS observation. Reservoir regulations may be one of the factors that alter the TWS signal.

In North China, annual precipitation in Hai River basin changed following a V-shaped process, with year 2006 as the turning point, which can also be recognized from the TWS estimates and water resources records. After rapid decline from 2004 to 2006 ($-2.48\,\mathrm{cm\,yr^{-1}}$), the TWS from the scaled GRACE data in Hai River basin became stable around 2007. Contrary to increasing precipitation, TWS dropped 3 cm in 2008 and continued to decline slowly at a rate of $-0.22\,\mathrm{cm\,yr^{-1}}$ until it started to recover in 2012. The TWS in Hai River basin generally showed a linear decreasing trend ($-1.27\,\mathrm{cm\,yr^{-1}}$) during 2004–2011. The residual between TWS from scaled GRACE data and the GLDAS ensemble mean could be treated approximately as the sum of surface reservoir and groundwater storage. Moreover, detection depth of GRACE is much deeper than the layers considered in models (1.9 m in VIC, 2.0 m in NOAH, 3.5 m in Mosaic and 3.43 m in CLM) and in field monitoring (shallow aquifer). Although the increasing precipitation seemed to have alleviated the depletion trend in these area, we shouldn't ignore the huge gap ($\sim -1.8\,\mathrm{cm\,yr^{-1}}$) between the trends of the time series of the residuals and summed water resources records (-1.28, $0.50\,\mathrm{cm\,yr^{-1}}$) during 2006–2011. The gap between these time series probably suggests that the long-term effect of over exploitation of groundwater still remained, even though water saving management practices had already been carried out in this basin, and water storage would suffer even worse depletion in the future drought years. Similar to Hai River basin, the TWS from scaled GRACE data in Yellow River basin followed a nearly linear decreasing trend ($-0.73\,\mathrm{cm\,yr^{-1}}$) during 2004–2011, and it changed more slowly ($-0.132\,\mathrm{cm\,yr^{-1}}$) after 2007. Disagreement between GRACE TWS, the TWS estimates and water resources records also revealed that there was an impact of human activities on the TWS variations in this basin. Over the recent decade, the TWS in Huai River basin showed a long-term descending trend ($-0.564\,\mathrm{cm\,yr^{-1}}$), which is similar to annual precipitation over this basin. The TWS from GLDAS ensemble mean also showed good agreement.

Annual variations in TWS from scaled GRACE data, the GLDAS ensemble mean and water resources records are more similar across basins in South China than they are in North China. The TWS in the Changjiang River basin, Zhujiang Basin and Southeast Rivers basin all followed an increasing trend from 2003 to 2013, at 0.348, 0.552 and 0.696 cm yr^{-1}, respectively. As a result of typhoons and tropical storms, the TWS in these basins also had much stronger fluctuations than in North China.

The TWS variations observed by GRACE are integrated information from different components in the vertical profile. Compared to water storage in surface soil layers, snow cover and canopy water storage are almost negligible in most regions, and correlation analysis results in China suggested that changes in soil moisture contributed significantly to TWSC (Table 5). The percentage of TWSC variance explained by SMC could be as high as 61.7 % at the national scale. In most basins, over half of the TWSC variance could be attributed to SMC, with high percentages in Changjiang basin and Zhujiang basin (63.9 and 67.1 %). In Heilongjiang River basin, SMC played a less important role in TWSC (38 %). Hydrologic fluxes fluctuations over the basin jointly affected water storage. According to correlation analysis based on GRACE TWS and GLDAS fluxes, precipitation, evapotranspiration and runoff each contributed 45.7, 40.8 and 32.1 %, respectively, of the TWSC variance in China (Table 5). As most basins we focused on are under control of the monsoon climate, precipitation and runoff generally showed higher contributions to the TWSC variance than evapotranspiration did. Overall, precipitation was found to have a much higher impact on TWSC in the south than in the north, with the highest explained variance in Zhujiang basin (59.9 %), followed by 43.6 % in Changjiang basin.

3.3 Spatial pattern of linear trend analysis

At a large scale, spatial patterns of linear trends calculated from scaled and unscaled GRACE TWS are consistent (Fig. 7a and c), but there are also some discrepancies at the small spatial scale and the former one seems to better correspond to natural features of the TWS intensity distribution, such as the absolute values of trends are

usually larger around river networks. From 2003 to 2013, four main regions were identified with intensive and significant long-term trends in TWS, and their performances were different in different seasons (Fig. 8).

According to the analysis in previous section, we inferred that human activities rather than climate parameters are responsible for the significant TWS depletion in North China, as withdrawals usually surpass net recharge in arid and semiarid regions. Severe areas mainly located in the Shanxi Province and south part in the Hebei Province, with decreasing trends less than –0.8 cm yr^{-1}. And offset to loss rate caused by mass gains from reservoir regulation, water diversion and coal transport in this region was estimated to 0.76 cm yr^{-1} (Tang et al., 2013). In the Shanxi Province, the east to mid-section of Yellow River, coal mining not only has disturbed normal recharge to the nearby aquifer but has also caused overexploitation of groundwater. The groundwater is a major source to water consumptions in Huang-Huai-Hai plain, where is intensively equipped with irrigation facility to withdraw freshwater from deep wells (Foster et al., 2004; Kendy et al., 2004). This poor condition deteriorates with seasons and the depletion becomes most severe, impacting the largest area in autumn. Considering irrigation demand concentrated mostly in MMA and high social water consumption comes with JJA, TWS probably needs time to show all this influence in SON. The Southwest rivers region (Yarlung Zangbo River, Nu River and Lancang River) also showed significant TWS depletion, particularly in the upstream and downstream portions of the Yarlung Zangbo River. The areas impacted by significant depletion was the largest in spring, while the depletion became the most severe in autumn. Climate observation across this region proved that annual precipitation was decreasing over 11 years, with significant droughts in 2006, 2009 and 2012. Moreover, previous research also find ice loss in Himalaya from 2003–2007 (Matsuo et al., 2010).

Along with increasing precipitation in Southeast China, there were significant increasing trends in TWS over the middle and lower reaches of the Changjiang and southeastern coastal areas. The main contribution to this significant increase occurred during the summer, when precipitation was the most concentrated of the year. There

are two places that showed significant TWS increases in the Tibetan plateau. One of these areas is around the Hoh Xil Mountains and the other is headstream region of the Yellow River; they have maximum increasing trends of 2.59 and 1.77 cm yr^{-1}, respectively. The Hoh Xil Mountains are located at the intersection of the inland lakes in the Qangtang plateau and the north source of the Changjiang River. Plateau's two largest freshwater lakes, Eling Lake and Zaling Lake, lie in the headstream region of the Yellow River. Previous research applied multi-source satellite data to reconstruct volume changes in the Tibetan plateau's major lakes, and found that they showed similar spatial distribution with mass variations in GRACE during 2003–2010 (Song et al., 2013). According to satellite images, lakes in Hoh Xil overall showed a trend of expansion during 2000–2011. Further analysis suggested that increasing precipitation and decreasing evaporation were major factors contributing to this trend, and additional water recharge from melting glacier and frozen soil caused by climate warming were minor factors (Yao et al., 2014; Duan et al., 2013). In the headstream region of the Yellow River, precipitation is the main recharge source to runoff, with a ratio of 63.15 %. Local observations revealed that there was an increasing trend in runoff as this region was becoming warmer and wetter during the period 2000–2012 (Lan et al., 2010, 2013; Wang et al., 2014). The Chinese government has launched an ecological protection and construction project in the Three River Sources that started in 2005. According to monitoring data from the Qinghai Provincial Meteorological Bureau, average lake extents during 2005–2012 showed an increase of 34.7 and 64.4 km^2 compared to those during 2003–2004 for Eling Lake and Zaling Lake, respectively.

In addition to above large areas, there are also some other small regions showing strong TWS changes from 2003 to 2013. Along the northeast country border, there is significant TWS increase ($0.34 \sim 1.19$ cm yr^{-1}), mostly is contributed by winter.The central part in Jilin Province in northeast China shows severe TWS depletion in autumn ($-1.10 \sim -2.28$ cm yr^{-1}), but those linear trends have not past significant test (P value < 0.05). In the northwest China, the unscaled GRACE data only shows significant water depletion mainly around Tianshan Mountains, which is also identified

with ice loss in previous research (Matsuo et al., 2010). But trends from the scaled GRACE TWS also illustrate significant TWS increase in the Turban basin, while depletion in its surrounding mountains. The Turban basin is the lowest basin in China, and Fig. 3b shows that the basin has much smaller TWS amplitude than that in surrounding mountains. Extreme arid climate and local topography feature in this region could make TWS more sensitive to climate change. Complex terrain in this region leads to more complicated GRACE TWS signal mixture at large spatial scale. Even though scale factors might have separated mixed TWS signals, limitations in factor's production should also be taken care of (Launderer et al., 2012). Thus, more data needs to be added to further quantify and verify the extent of identified TWS change at small scale in the future research.

4 Summary and conclusions

In this study we analyzed annual variations in TWS over 11 years in China and eight of its basins, based on scaled GRACE data in combination with GLDAS simulations and water resources records. Areas with significant long-term trends were also identified and discussed. The major points are summarized as follows:

1. Gridded scale factors could adequatelly correct leakage errors in the GRACE products and the scaled data gained more spatial details of the TWS intensity distribution. The values of the regionally averaged TWS were amplified after scale factors were applied. These increase percentages reached up to over 50 % in Huai River basin (57.2 %) and Zhujiang basin (53.6 %), but were tiny for basins with larger sizes, such as Liao River basin (9.5 %) and Yellow River basin (8 %).

2. The TWS at the national scale stayed at a relatively low level. These values exhibited high intensity variations from 2006 to 2012, before recovering to their 2003 to 2005 condition. The TWS in the Hai River basin, Huai River basin and Yellow River basin almost decreased linearly while it increased in fluctuations in the

Changjiang basin, Zhujiang basin and Southeast Rivers basin. The TWS variations generally followed the variations in annual precipitation, but depletion in deep aquifers caused by overexploitation played a significant role in these trends until 2012 in the Hai River basin and Yellow River basin.

3. Changes in soil moisture storage contributed 61.7 % of the TWSC variance at the national scale, and the percentages were generally beyond 50 % in all basins with exceptions in Heilongjiang River basin (38 %) and Yellow River basin (46.3 %). Under the control of the monsoon climate, precipitation and runoff explained more variance in TWSC than evapotranspiration did, and precipitation's ability to explain TWSC variations was stronger in the south basins than in the north, reaching up to 59.9 % in Zhujiang basin.

4. From 2003 to 2013, there were significant water storage depletions over the Southwest rivers region and North China, and the areas that exhibited significant depletions were the largest in spring and summer, respectively. The middle and lower reaches of Changjiang and southeastern coastal areas, as well as the Hoh Xil Mountains, and the headstream region of the Yellow River in the Tibetan plateau, all exhibited significant increases in TWS. These identified trends reflected TWS's responses to regional climate changes and human activities.

The current data period of GRACE products is shorter than some existing remote sensing data sets or site records, and the resolution and accuracy of GRACE data also need to be improved. However, TWS from GRACE has proved to be valuable to understanding large-scale hydrological process over land. The results in this study would be helpful for water resources management and climate change impact research. More sources of data will be added to further analyze regions or phenomena addressed in this study. The GRACE Follow On mission has already been scheduled, and will continue to support monitoring and research on TWS in the future.

Acknowledgements. This research received financial support from the International Science & Technology Cooperation Program of China (grant number: 2013DFG21010). The GLDAS simulations were provided by Goddard Earth Sciences (GES) Data and Information Services Center (DISC) (http://disc.sci.gsfc.nasa.gov/services/disc/services/grads-gds/gldas). GRACE land data (available at http://grace.jpl.nasa.gov) processing algorithms were provided by Sean Swenson, and supported by the NASA MEaSUREs Program. The authors would also like to thank the anonymous reviewers for the valuable comments that helped to improve the manuscript.

References

Andersen, O. B., Seneviratne, S. I., Hinderer, J., and Viterbo, P.: GRACE-derived terrestrial water storage depletion associated with the 2003 European heat wave, Geophys. Res. Lett., 32, L18405, doi:10.1029/2005GL023574, 2005.

Betts, A. K., Chen, F., Mitchell, K., and Janjic, Z. I.: Assessment of the land surface and boundary layer models in two operational versions of the NCEP Eta model using FIFE data, Mon. Weather Rev., 125, 2896–2916, 1997.

Bonan, G. B., Oleson, K. W., Vertenstein, M., Levis, S., Zeng, X. B., Dai, Y. J., Dickinson, R. E., and Yang, Z. L.: The land surface climatology of the NCAR Land Surface Model coupled to the NCAR Community Climate Model, J. Climate, 11, 1307–1326, 1998.

Chen, F., Mitchell, K., Schaake, J., Xue, Y. K., Pan, H. L., Koren, V., Duan, Q. Y., Ek, M., and Betts, A.: Modeling of land-surface evaporation by four schemes and comparison with FIFE observations, J. Geophys. Res., 101, 7251–7268, 1996.

Chen, J. L., Wilson, C. R., Famiglietti, J. S., and Rodell, M.: Attenuation effect on seasonal basin-scale water storage changes from GRACE time-variable gravity, J. Geodesy., 81, 237–245, 2007.

Chen, J. L., Wilson, C. R., Tapley, B. D., Yang, Z. L., and Niu, G. Y.: The 2005 drought event in the Amazon River basin as measured by GRACE and estimated by climate models, J. Geophys. Res., 114, B05404, doi:10.1029/2008JB006056, 2009.

Chen, J. L., Li, J., Zhang, Z. Z., and Ni, S. N.: Long-term groundwater variations in Northwest India from satellite gravity measurements, Global Planet. Change, 116, 130–138, 2014.

Crowley, J. W., Mitrovica, J. X., Bailey, R. C., Tamisiea, M. E., and Davis, J. L.: Annual variations in water storage and precipitation in the Amazon Basin, J. Geodesy., 82, 9–13, 2008.
Dai, Y. J. and Zeng, Q. C.: A land surface model (IAP94) for climate studies, Part I: Formulation and validation in off-line experiments, Adv. Atmos. Sci., 14, 443–460, 1997.
Dickinson, R. E., Henderson-Sellers, A., and Kennedy, P. J.: Biosphere–atmosphere Transfer Scheme (BATS) Version 1e as Coupled to the NCAR Community Climate Model, NCAR Technical Note NCAR/TN-387+STR, NCAR, doi:10.5065/D67W6959, 1993.
Duan, J. B., Zhong, M., Yan, W. M., and Jiang, M.: Recovery of land water storage variations in Chinese mainland by use of grace data, J. Geodesy., 27, 68–71, 2007.
Ek, M. B., Mitchell, K. E., Lin, Y., Rogers, E., Grunmann, P., Koren, V., Gayno, G., and Tarpley, J. D.: Implementation of Noah land surface model advances in the National Centers for Environmental Prediction operational mesoscale Eta model, J. Geophys. Res., 108, 8851, doi:10.1029/2002JD003296, 2003.
Famiglietti, J. S.: Remote sensing of terrestrial water storage, soil moisture and surface waters, in: The State of the Planet: Frontiers and Challenges in Geophysics, edited by: Sparks, R. S. J. and Hawkesworth, C. J., American Geophysical Union, Washington, D.C., 197–207, 2004.
Famiglietti, J. S., Lo, M., Ho, S. L., Bethune, J., Anderson, K. J., Syed, T. H., Swenson, S. C., de Linage, C. R., and Rodell, M.: Satellites measure recent rates of groundwater depletion in California's Central Valley, Geophys. Res. Lett., 38, L03403, doi:10.1029/2010GL046442, 2011.
Feng, W., Zhong, M., Lemoine, J. M., Biancale, R., Hsu, H. T., and Xia, J.: Evaluation of groundwater depletion in North China using the Gravity Recovery and Climate Experiment (GRACE) data and ground-based measurements, Water Resour. Res., 49, 2110–2118, 2013.
Foster, S., Garduno, H., Evans, R., Olson, D., Tian, Y., Zhang, W. Z., and Han, Z. S.: Quaternary aquifer of the North China Plain – assessing and achieving groundwater resource sustainability, Hydrogeol. J., 12, 81–93, 2004.
Hirschi, M., Seneviratne, S. I., and Schar, C.: Seasonal variations in terrestrial water storage for major mid-latitude river basins, J. Hydrometeorol., 7, 39–60, 2006.
Hu, X. G., Chen, J. L., Zhou, Y. H., Cheng, H., and Liao, X. H.: Seasonal water storage change of the Yangtze River Basin detected by GRACE, Sci. China Ser. D, 49, 483–491, 2006.
Jin, S. G. and Feng, G. P.: Large-scale variations of global groundwater from satellite gravimetry and hydrological models, 2002–2012, Global Planet. Change, 106, 20–30, 2013.

Kendy, E., Zhang, Y. Q., Liu, C. M., Wang, J. X., and Steenhuis, T.: Groundwater recharge from irrigated cropland in the North China Plain: case study of Luancheng County, Hebei Province, 1949–2000, Hydrol. Process., 18, 2289–2302, 2004.
Kim, H., Pat Yeh, J. F., Oki, T., and Kanae, S.: Role of rivers in the seasonal variations of terrestrial water storage over global basins, Geophys. Res. Lett., 36, L17402, doi:10.1029/2009GL039006, 2009.
Koren, V., Schaake, J., Mitchell, K., Duan, Q. Y., Chen, F., and Baker, J. M.: A parameterization of snowpack and frozen ground intended for NCEP weather and climate models, J. Geophys. Res., 104, 19569–19585, 1999.
Koster, R. D. and Suarez, M. J.: Energy and Water Balance Calculations in the Mosaic LSM, NASA Technical Memorandum 104606, NASA, http://citeseerx.ist.psu.edu/viewdoc/summary?doi=10.1.1.25.8609 (last access: May 2015), 1996.
Lan, Y. C., Zhao, G. H., Zhang, Y. N., Wen, J., Liu, J. Q., and Hu, X. L.: Response of runoff in the source of the Yellow River to climate warming, Quatern. Int., 226, 60–65, 2010.
Lan, Y. C., Lu, C. Y., La, C. F., Sheng, Y. P.: The factor of climate shift to warm-humid in the source regions of the Yellow River and its hydrologic response, J. Glaciol. Geocryl., 35, 920–928, 2013.
Landerer, F. W. and Swenson, S. C.: Accuracy of scaled GRACE terrestrial water storage estimates, Water Resour. Res., 48, W04531, doi:10.1029/2011WR011453, 2012.
Landerer, F. W., Dickey, J. O., and Gntner, A.: Terrestrial water budget of the Eurasian pan-Arctic from GRACE satellite measurements during 2003–2009, J. Geophys. Res., 115, D23115, doi:10.1029/2010JD014584, 2010.
Leblanc, M. J., Tregoning, P., Ramillien, G., Tweed, S. O., and Fakes, A.: Basin-scale, integrated observations of the early 21st century multiyear drought in southeast Australia, Water Resour. Res., 45, W04408, doi:10.1029/2008WR007333, 2009.
Lettenmaier, D. P. and Famiglietti, J. S.: Water from on high, Nature, 444, 562–563, 2006.
Liang, X., Lettenmaier, D. P., Wood, E. F., and Burges, S. J.: A simple hydrologically based model of land surface water and energy fluxes for GSMs, J. Geophys. Res., 99, 14415–14428, 1994.
Liang, X., Lettenmaier, D. P., and Wood, E. F.: One-dimensional statistical dynamic representation of subgrid spatial variability of precipitation in the two-layer variable infiltration capacity model, J. Geophys. Res., 101, 21403–21422, 1996.

Long, D., Scanlon, B. R., Longuevergne, L., Sun, A. Y., Fernando, D. N., and Save, H.: GRACE satellites monitor large depletion in water storage in response to the 2011 drought in Texas, Geophys. Res. Lett., 40, 3395–3401, 2013.

Matsuo, K. and Heki, K.: Time-variable ice loss in Asian high mountains from satellite gravimetry, Earth Planet. Sc. Lett., 290, 30–36, 2010.

Moiwo, J. P., Yang, Y., Li, H., Han, S., and Hu, Y.: Comparison of GRACE with in situ hydrological measurement data shows storage depletion in Hai River Basin, northern China, Water SA, 35, 663–670, 2009.

Oleson, K. W., Niu, G. Y., Yang, Z. L., Lawrence, D. M., Thornton, P. E., Lawrence, P. J., Stöckli, R., Dickinson, R. E., Bonan, G. B., Levis, S., Dai, A., and Qian, T.: Improvements to the community land model and their impact on the hydrological cycle, J. Geophys. Res., 113, G01021, doi:10.1029/2007JG000563, 2008.

Rodell, M. and Famiglietti, J. S.: Detectability of variations in continental water storage from satellite observations of the time dependent gravity field, Water Resour. Res., 35, 2705–2723, 1999.

Rodell, M. and Famiglietti, J. S.: An analysis of terrestrial water storage variations in Illinois with implications for the Gravity Recovery and Climate Experiment (GRACE), Water Resour. Res., 37, 1327–1339, 2001.

Rodell, M., Houser, P. R., Jambor, U., Gottschalck, J., Mitchell, K., Meng, C. J., Arsenault, K., Cosgrove, B., Radakovich, J., Bosilovich, M., Entin, J. K., Walker, J. P., Lohmann, D., and Toll, D.: The Global Land Data Assimilation System, B. Am. Meteorol. Soc., 85, 381–394, 2004.

Rodell, M., Velicogna, I., and Famiglietti, J. S.: Satellite-based estimates of groundwater depletion in India, Nature, 460, 999–1002, 2009.

Sakumura, C., Bettadpur, S., and Bruinsma, S.: Ensemble prediction and intercomparison analysis of GRACE time-variable gravity field models, Geophys. Res. Lett., 41, 1389–1397, 2014.

Schmidt, R., Schwintzed, P., Flechtner, F., Reigbera, C., Güntnera, A., Döllb, P., Ramillienc, G., Cazenavec, A., Petrovica, S., Jochmanna, H., and Wünsch, J.: GRACE observations of changes in continental water storage, Global Planet. Change, 50, 112–126, 2006.

Song, C. Q., Huang, B., and Ke, L. H.: Modeling and analysis of lake water storage changes on the Tibetan Plateau using multi-mission satellite data, Remote Sens. Environ., 135, 25–35, 2013.

Strassberg, G., Scanlon, B. R., and Rodell, M.: Comparison of seasonal terrestrial water storage variations from GRACE with groundwater-level measurements from the High Plains Aquifer (USA), Geophys. Res. Lett., 34, L14402, doi:10.1029/2007GL030139, 2007.

Su, X. L., Ping, J. S., and Ye, Q. X.: Terrestrial water variations in the North China Plain revealed by the GRACE mission, Sci. China Earth Sci., 54, 1965–1970, 2011.

Swenson, S. C. and Wahr, J.: Monitoring changes in continental water storage with GRACE, Space Sci. Rev., 108, 345–354, 2003.

Swenson, S. C. and Wahr, J.: Post-processing removal of correlated errors in GRACE data, Geophys. Res. Lett., 33, L08402, doi:10.1029/2005GL025285, 2006.

Syed, T. H., Lakshmi, V., Paleologos, E., Lohmann, D., Mitchell, K., and Famiglietti, J. S.: Analysis of process controls in land surface hydrological cycle over the continental United States, J. Geophys. Res., 109, 1–11, 2004.

Syed, T. H., Famiglietti, J. S., Chen, J. L., Rodell, M., Seneviratne, S. I., Viterbo, P., and Wilson, C. R.: Total basin discharge for the Amazon and Mississippi river basins from GRACE and a land–atmosphere water balance, Geophys. Res. Lett., 32, L24404, doi:10.1029/2005GL024851, 2005.

Syed, T. H., Famiglietti, J. S., Rodell, M., Chen, J. L., and Wilson, C. R.: Analysis of terrestrial water storage changes from GRACE and GLDAS, Water Resour. Res., 44, W02433, doi:10.1029/2006WR005779, 2008.

Tang, J. S., Cheng, H. W., and Liu, L.: Assessing the recent droughts in Southwestern China using satellite gravimetry, Water Resour. Res., 50, 3030–3038, 2014.

Tang, Q. H., Zhang, X. J., and Tang, Y.: Anthropogenic impacts on mass change in North China, Geophys. Res. Lett., 40, 3924–3928, 2013.

Tapley, B., Bettadpur, S., Ries, J., Thompson, P., and Watkins, M.: GRACE measurements of mass variability in the Earth system, Science, 305, 503–505, 2004.

Wahr, J., Swenson, S. C., Zlotnicki, V., and Velicogna, I.: Time-variable gravity from GRACE: first results, Geophys. Res. Lett., 31, L11501, doi:10.1029/2004GL019779, 2004.

Wang, C. and Yang, T.: Spatial–temporal characteristics of terrestrial water storage variation in China base on GRACE satellite data, Water Resour. Power, 31, 20–23, 2013.

Wang, H., Li, D. L., and Jiang, Y. C.: Characteristics and reasons of the runoff variation in source regions of the Yellow River during 1956–2012, J. Glaciol. Geocryol., 36, 403–412, 2014.

Xie, P. and Arkin, P. A.: Global precipitation: a 17-year monthly analysis based on gaugeobservations, satellite estimates, and numerical model outputs, B. Am. Meteorol. Soc., 78, 2539–2558, 1996.

Xu, M., Ye, B. S., and Zhao, Q. D.: Temporal and spatial pattern of water storage changes over the Yangtz river basin during 2002–2010 based on GRACE satellite data, Prog. Geogr., 32, 68–77, 2013.

Yao, X. J., Liu, S. Y., Li, L., Sun, M. P., and Luo, J.: Spatial–temporal characteristics of lake area variations in Hoh Xil region from 1970 to 2011, J. Geogr. Sci., 24, 689–702, 2014.

Yirdaw, S. Z., Snelgrove, K. R., and Agboma, C. O.: GRACE satellite observations ofterrestrial moisture changes for drought characterization in the Canadian Prairie, J. Hydrol., 356, 84–92, 2008.

Zeng, N., Yoon, J. H., Mariotti, A., and Swenson, S.: Variability of basin-scale terrestrial water storage from a P-E-R water budget method: the Amazon and the Mississippi, J. Climate, 21, 248–265, 2008.

Zhong, M., Duan, J. B., Xu, H. Z., Peng, P., Yan, H. M., and Zhu, Y. Z.: Trend of China land water storage redistribution at medi- and large-spatial scales in recent five years by satellite gravity observations, Chinese Sci. Bull., 54, 816–821, 2009.

Table 1. Variables used in the GLDAS simulations.

GLDAS Variables	Units	Temporal resolution	Spatial resolution
Soil moisture	$kg\,m^{-2}$	Monthly	$1^{\circ} \times 1^{\circ}$
Snow water equivalent	$kg\,m^{-2}$	Monthly	$1^{\circ} \times 1^{\circ}$
Canopy water storage	$kg\,m^{-2}$	Monthly	$1^{\circ} \times 1^{\circ}$
Precipitation	$kg\,m^{-2}\,s^{-1}$	Monthly	$1^{\circ} \times 1^{\circ}$
Evapotranspiration	$kg\,m^{-2}\,s^{-1}$	Monthly	$1^{\circ} \times 1^{\circ}$
Runoff	$kg\,m^{-2}\,s^{-1}$	Monthly	$1^{\circ} \times 1^{\circ}$

Table 2. Correlation coefficients between regionally averaged TWS from the scaled GRACE data and model simulations in China and eight of its basins. Bold numbers highlight the best model result in each region.

Region	CLM	VIC	MOSAIC	NOAH	Ensemble mean
HLJ	0.83	0.84	0.74	**0.87**	0.86
LR	**0.71**	0.65	0.54	0.64	0.64
HaiR	0.43	0.54	**0.66**	0.61	0.61
HuaiR	0.68	0.54	0.68	**0.79**	0.72
YR	**0.77**	0.62	0.62	0.70	0.69
CJ	0.61	0.51	0.47	**0.77**	0.60
ZJ	0.70	0.77	0.79	**0.82**	0.81
SERs	0.70	0.69	**0.83**	0.76	0.81
CHN	0.25	0.31	0.53	**0.79**	0.55

Table 3. Error statistics of regionally averaged TWS (unit: cm).

Regions	Areas (km^2)	Measurement error	Leakage error	Total error	Bias for GLDAS
China	9 510 610	0.380	0.312	0.537	0.629
Changjiang	1 815 855	0.900	0.793	1.273	1.470
Heilongjiang	956 832	0.980	0.719	1.386	1.095
Yellow River	860 883	0.776	0.733	1.097	0.720
Zhujiang	463 050	1.861	1.621	2.632	3.347
Hai River	327 096	1.301	1.364	1.840	1.591
Liao river	310 881	1.132	0.984	1.601	1.605
Huai River	288 152	1.742	1.535	2.463	3.514
Southeast Rivers	242 524	1.440	1.287	2.037	3.692

Table 4. Slopes of the fitting for the basin-averaged TWS from the scaled and the unscaled GRACE data.

Region	HLJ	LR	HaiR	HuaiR	YR	CJ	ZJ	SERs	CHN
factor	1.256	1.095	1.315	1.572	1.080	1.338	1.536	1.107	1.188
R^2	0.996	0.989	0.988	0.994	0.982	0.992	0.996	0.991	0.982

Table 5. Coefficient of determination R^2 between precipitation (P), evapotranspiration (E), runoff (Q), soil moisture change (SMC) from GLDAS ensemble mean and TWSC from the scaled GRACE data in 2003–2013.

	HLJ	LR	HaiR	HuaiR	YR	CJ	ZJ	SERs	CHN
P	0.039	0.195	0.180	0.347	0.408	0.436	0.599	0.225	0.457
E	0.001	0.082	0.102	0.089	0.281	0.245	0.301	0.000	0.321
Q	0.082	0.263	0.291	0.310	0.384	0.466	0.504	0.181	0.408
SMC	0.380	0.522	0.527	0.571	0.463	0.639	0.671	0.508	0.671

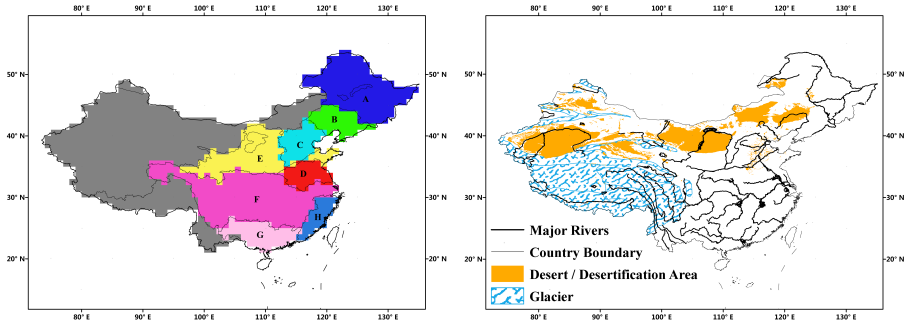

Figure 1. Schematic diagrams of research area (A: Heilongjiang River; B: LiaoRiver; C: HaiRiver; D: HuaiRiver; E: YellowRiver; F: Changjiang; G: Zhujiang; H: Southeast Rivers).

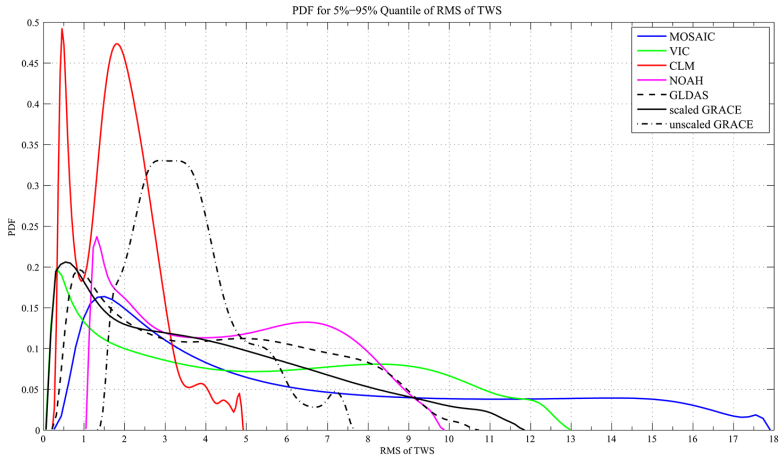

Figure 2. Empirical probability density distributions of root-mean-square of TWS from the scaled GRACE data, the unscaled GRACE data and model simulations (only TWS values between the 5th and 95th quantiles are considered), unit of RMS is cm.

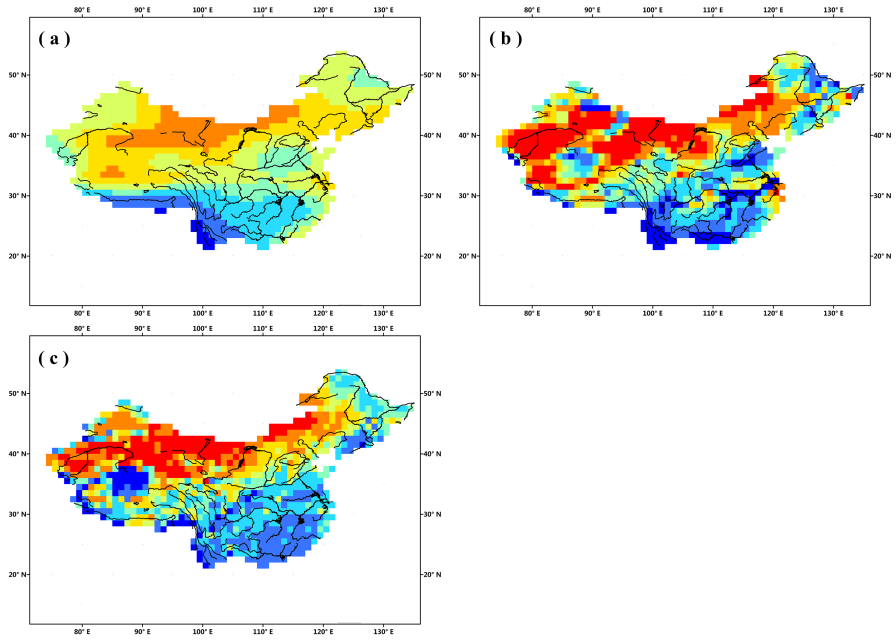

Figure 3. Root-mean-square of TWS from the unscaled GRACE data **(a)**, the scaled GRACE data **(b)** and the GLDAS ensemble mean **(c)** (unit: cm).

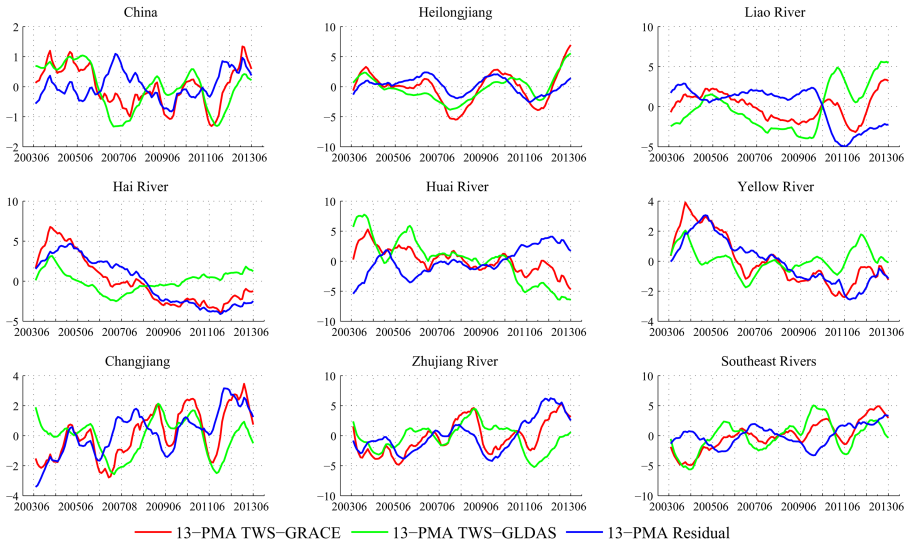

Figure 4. Regionally averaged TWS time series (2003–2013) from the scaled GRACE data and the GLDAS ensemble mean, and their residual time series for China and eight of its basins (all time series have been processed with 13-point moving average; unit: cm).

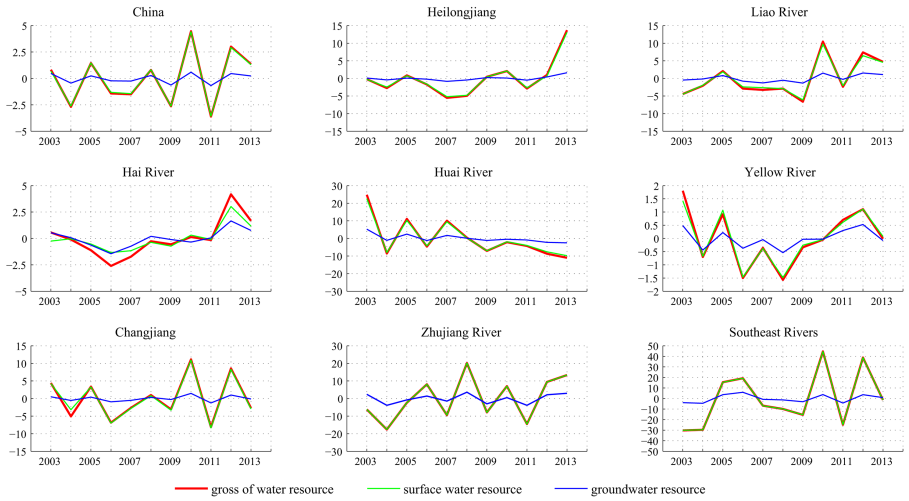

Figure 5. Annual variations of water resources in China and eight of its basins from 2003–2013 (multi-year average has been subtracted from all values; unit: cm).

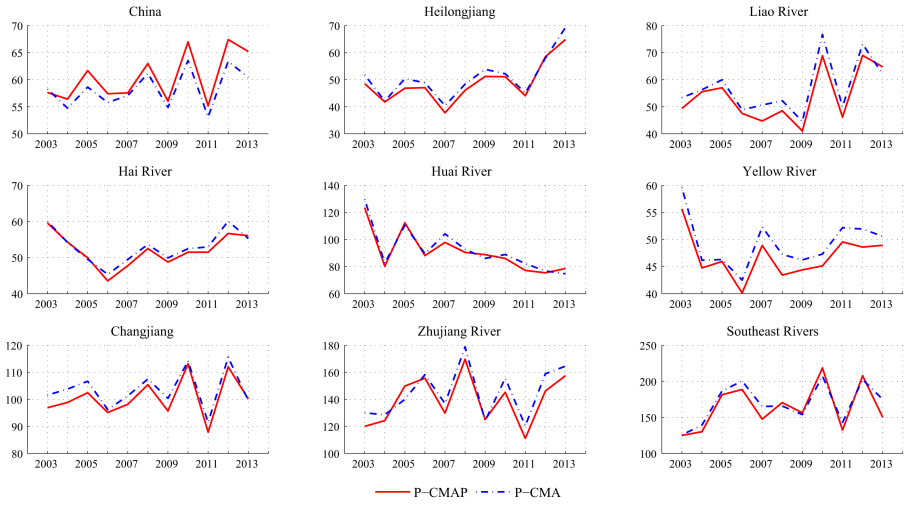

Figure 6. Regionally average annual precipitation for China and eight of its basins from 2003–2013 (unit: cm). P-CMAP refers to precipitation grid data from GLDAS forcing, and P-CMA refers to precipitation grid data from station observation offered by China Meteorological Administration.

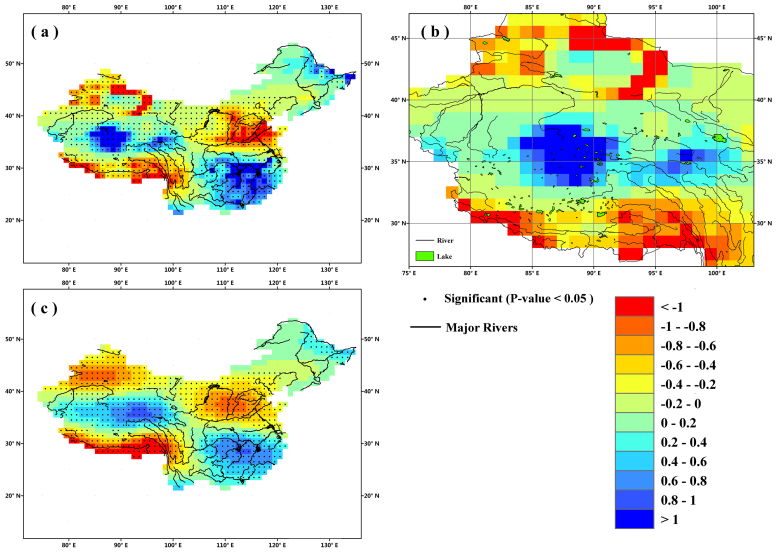

Figure 7. Spatial distribution of linear trends for TWS in 2003–2013 (unit: cm yr^{-1}); **(a)** and **(b)** are linear trends from the scaled GRACE data and its detailed diagram for west part of China, **(c)** is linear trend from the unscaled GRACE data.

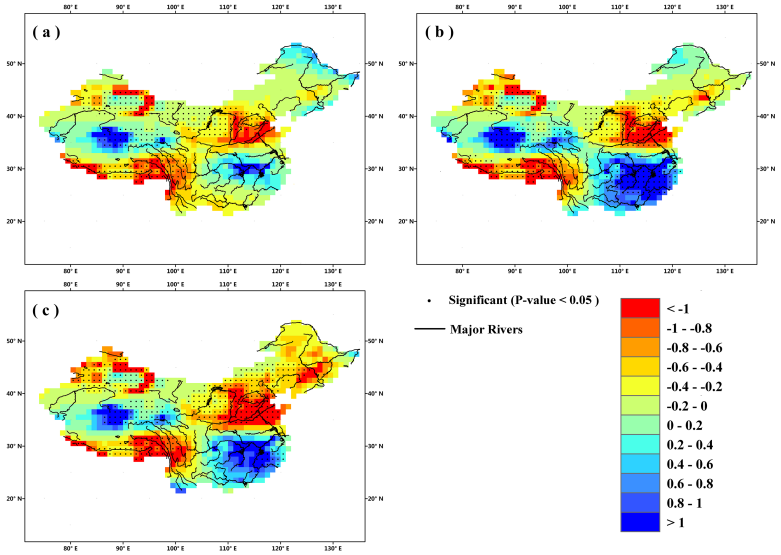

Figure 8. Spatial distribution of linear trends for the seasonal averaged TWS in 2003–2013 from the scaled GRACE data (unit: cm yr^{-1}); **(a)** spring; **(b)** summer; **(c)** autumn.